Aberrant brain oscillatory coupling from the primary motor cortex in children with autism spectrum disorders

Kyung-min An [a,b,*], Takashi Ikeda [a,b], Chiaki Hasegawa [a], Yuko Yoshimura [a,b,c], Sanae Tanaka [a,b], Daisuke N. Saito [a,b], Ken Yaoi [a,b], Sumie Iwasaki [a], Tetsu Hirosawa [a,b], Ole Jensen [e], Mitsuru Kikuchi [a,b,d,*]

[a] Research Center for Child Mental Development, Kanazawa University, Kanazawa, Japan
[b] Division of Socio-Cognitive-Neuroscience, Department of Child Development United Graduate School of Child Development, Osaka University, Kanazawa University, Hamamatsu University School of Medicine, Chiba University and University of Fukui, Kanazawa, Japan
[c] Institute of Human and Social Sciences, Kanazawa University, Kanazawa, Japan
[d] Department of Psychiatry and Behavioral Science, Kanazawa University, Kanazawa, Japan
[e] Centre for Human Brain Health, School of Psychology, University of Birmingham, United Kingdom

ARTICLE INFO

ABSTRACT

Autism spectrum disorder (ASD) often involves dysfunction in general motor control and motor coordination, in addition to core symptoms. However, the neural mechanisms underlying motor dysfunction in ASD are poorly understood. To elucidate this issue, we focused on brain oscillations and their coupling in the primary motor cortex (M1). We recorded magnetoencephalography in 18 children with ASD, aged 5 to 7 years, and 19 age- and IQ-matched typically-developing children while they pressed a button during a video-game-like motor task. The motor-related gamma (70 to 90 Hz) and pre-movement beta oscillations (15 to 25 Hz) were analyzed in the primary motor cortex using an inverse method. To determine the coupling between beta and gamma oscillations, we applied phase-amplitude coupling to calculate the statistical dependence between the amplitude of fast oscillations and the phase of slow oscillations. We observed a motor-related gamma increase and a pre-movement beta decrease in both groups. The ASD group exhibited a reduced motor-related gamma increase and enhanced pre-movement beta decrease in the ipsilateral primary motor cortex. We found phase-amplitude coupling, in which high-gamma activity was modulated by the beta rhythm in the primary motor cortex. Phase-amplitude coupling in the ipsilateral primary motor cortex was reduced in the ASD group compared with the control group. Using oscillatory changes and their couplings, linear discriminant analysis classified the ASD and control groups with high accuracy (area under the receiver operating characteristic curve: 97.1%). The current findings revealed alterations in oscillations and oscillatory coupling, reflecting the dysregulation of motor gating mechanisms in ASD. These results may be helpful for elucidating the neural mechanisms underlying motor dysfunction in ASD, suggesting the possibility of developing a biomarker for ASD diagnosis.

1. Introduction

Autism spectrum disorder (ASD) is a neurological developmental disorder characterized by persistent deficits in social interaction and communication, and the presence of repetitive behaviors with restricted interests (American Psychiatric Association, 2013). In addition to the core symptoms of ASD, previous studies have reported that children and adults with ASD often exhibit significant motor dysfunction (Teitelbaum et al., 1998; Lord et al., 2000; Fournier et al., 2010; Lloyd et al., 2013).

Kanner (1943), who proposed the first clear definition of autism, included motor dysfunction as a symptom of ASD (Kanner, 1943). Motor abnormalities have been widely reported in ASD, involving fine and gross motor skills, gait, balance, and posture (Lord et al., 2000; Noterdaeme et al., 2002; Molloy et al., 2003; Jansiewicz et al., 2006; Bryson et al., 2007; Fournier et al., 2010; Lloyd et al., 2013; Radonovich et al., 2013). Although motor dysfunction is excluded from current diagnostic criteria for ASD, several recent studies have suggested that motor abnormalities should be considered as a core symptom of ASD (Fournier

et al., 2010; Lloyd et al., 2013; London, 2014).

Brain oscillations are rhythmic patterns of neural activity, and motor control modulates typical brain oscillations, particularly in the beta (13–30 Hz) and gamma frequency bands (60–90 Hz). Gamma oscillations are known to increase immediately after movement onset, and motor-related gamma oscillations are thought to be associated with motor execution and initiation (Pfurtscheller et al., 2003; Cheyne et al., 2008; Muthukumaraswamy, 2010; Cheyne and Ferrari, 2013). In addition, the power of beta oscillations begins to decrease prior to movement onset and is maintained during movement execution; these beta decreases are thought to be related to motor planning and movement preparation (Pfurtscheller and Lopes da Silva, 1999; Pfurtscheller et al., 2003; Doyle et al., 2005; Bai et al., 2011). In a previous study, we found that motor-related gamma oscillations were decreased in children with ASD, suggesting a potential biomarker for ASD using gamma oscillatory changes as a neurophysiological index and button response time as a behavioral index (An et al., 2018). However, pre-movement and movement-related beta oscillations have not been well characterized in ASD. Thus, in the present study, we investigated whether motor dysfunction in ASD is reflected by alterations in not only motor-related gamma oscillations but also pre-movement and movement-related beta oscillations.

Recently, there has been increasing research interest in the coupling between brain oscillations, with several studies reporting that the particular phase of a low-frequency rhythm modulates the amplitude of high-frequency brain activity in several brain areas (Canolty et al., 2006; Jensen and Colgin, 2007; Canolty and Knight, 2010; Hyafil et al., 2015). This type of phase-amplitude coupling (PAC) plays a functional role in local brain connectivity, coordinating the timing of neural activity in brain networks. Individuals with ASD have been reported to exhibit reduced PAC during visual grating tasks (Seymour et al., 2019) and face recognition tasks (Khan et al., 2013; Mamashli et al., 2018). Reduced PAC in ASD has been suggested to be related to dysregulation of local connectivity during sensory processing. However, PAC during motor control in ASD is poorly understood.

Previous electrocorticogram (ECoG) studies (de Hemptinne et al., 2013, 2015) reported that the amplitude of high-gamma activity is modulated by the phase of beta rhythms in the primary motor cortex (M1). PAC from M1 has been suggested as a crucial gating mechanism for movement execution, and exaggerated PAC has been shown in patients with movement disorders such as Parkinson's disease (de Hemptinne et al., 2013, 2015). We speculate that, in individuals with ASD, beta-high gamma coupling from M1 might be reduced, as in the visual sensory system of individuals with ASD. Alternatively, beta-high gamma coupling from M1 might be exaggerated, as in patients with Parkinson's disease. Aberrant M1 PAC in individuals with ASD may reflect the mechanisms underlying motor dysfunction. Importantly, previous studies have only investigated PAC from M1 using invasive brain recording techniques. Thus, we sought to investigate PAC from M1 using magnetoencephalography (MEG) as a non-invasive neuroimaging method.

In the present study, we measured beta-gamma PAC from M1 in children using child-customized MEG. We hypothesized that beta-high gamma PAC from M1 would be altered (either reduced or exaggerated) in children with ASD. In addition, we investigated whether beta and gamma oscillations during motor control were altered in ASD.

2. Materials and methods

2.1. Participants

Eighteen children with ASD (mean age = 6.00 years, SD = 0.59; five females) and 19 age-matched typically-developing (TD) children (mean age = 5.71 years, SD = 0.46, four females) participated in this study (Table 1). We used data from 14 children with ASD and 15 TD children collected in our previous study (An et al., 2018), as well as data from

Table 1
Participants' characteristics.

	TD	ASD	t	p	Cohen's d
Sex (male/female)	15 / 4	13 / 5			
Age (months)	68.53 ± 5.56	72.00 ± 7.10	−1.662	0.105	−0.547
K-ABC achievement score	104.21 ± 13.34	96.94 ± 17.23	1.439	0.159	0.473
ADOS total score	–	5.17 ± 1.38			

Means ± SDs and accompanying statistics (two-sided t-tests) of participants' characteristics. Significant differences in age and intelligence were not observed between the TD and ASD groups. K-ABC = Kaufman Assessment Battery for Children; ADOS = Autism Diagnostic Observation Schedule.

four additional children with ASD and four additional TD children. All participants were identified as right-handed using the Edinburgh Handedness Inventory (Oldfield, 1971). The Ethics Committee of the Kanazawa University Hospital approved this study, and parents of all participants provided full written informed consent.

Participants with ASD had confirmed diagnoses of ASD based on DSM-V criteria for autism or Asperger's syndrome (American Psychiatric Association, 2013), the Diagnostic Interview for Social and Communication Disorders (Wing et al., 2002), and/or the Autism Diagnostic Observational Schedule, Generic (ADOS) (Lord et al., 2000).

Intelligence was assessed using the Kaufman Assessment Battery for Children (K-ABC), and there was no significant difference in achievement scores between the two groups (t(35) = 1.439, p = 0.159, Cohen's d = 0.473).

Means ± SDs and accompanying statistics (two-sided t-tests) of participants' characteristics. Significant differences in age and intelligence were not observed between the TD and ASD groups. K-ABC = Kaufman Assessment Battery for Children; ADOS = Autism Diagnostic Observation Schedule.

2.2. Experimental paradigm

To investigate motor-related oscillatory changes and oscillatory coupling, we used a video-game-like motor task developed in our previous study (An et al., 2018). The experimental paradigm for the video-game-like motor task is shown in Fig. 1A. The motor task contained 10 blocks and involved 100 button presses. The aim of this motor task is to help a puppy collect fruit by pressing a button. Participants were instructed to gaze at a fixation point in the middle of the screen. When the fruit appeared at the fixation point, participants were instructed to press the button using their right index finger. When the button was pressed, the puppy jumped and caught the fruit. Fruit targets randomly appeared every 3.5 to 4.5 s after each button response. Each block contained 10 trials, and a bone with a red ribbon was obtained as a reward for successfully completing each block.

We designed this motor task to minimize participants' eye movement by presenting a fixation point in the middle of the screen. To calculate response time, we instructed participants to press the button as quickly as possible. Button responses were measured using a non-magnetic fiber optic response pad (LUMINA LU400-PAIR, Cedrus Corporation, San Pedro, CA, USA).

MEG was recorded for approximately 9 min (100 button presses) during the motor task. The visual stimuli were presented on a screen (26° × 21° of visual angle) using an LCD projector (IPSiO PJWX6170N, Ricoh Company, Ltd., Tokyo, Japan).

2.3. Magnetoencephalography recording

MEG data were acquired using a whole-head 151-channel child-customized MEG system (PQ 1151 R, Yokogawa/KIT, Kanazawa,
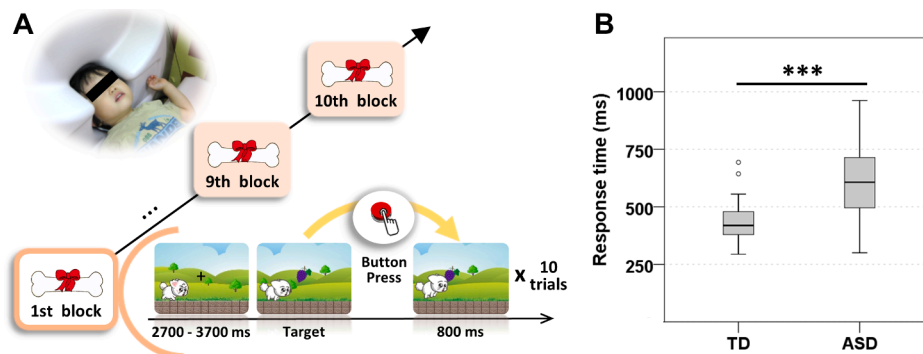
Fig. 1. Experimental paradigm and button response time in the TD and ASD groups. **A.** Children performed a video-game-like motor task. The motor task consisted of 10 blocks, and a bone with a red ribbon was given as a reward in the game after each block was successfully completed. The participants helped a puppy obtain fruit targets, and the action was repeated 10 times in each block. The target appeared every 3500 to 4500 ms. Before the target appeared, participants were asked to pay attention to the fixation point. After the target appeared at the fixation point, participants were asked to press the button as quickly as possible. When the participant pressed the button, the puppy jumped and obtained a fruit target. **B.** The button response time was calculated by subtracting the timing of the target from the timing of the button press. The median is shown as a line in the center of the box. The ASD group exhibited a significantly prolonged button response time compared with the TD group. (For interpretation of the references to colour in this figure legend, the reader is referred to the web version of this article.)

Japan) in a magnetically shielded room. MEG signals were digitized at 2000 Hz and low-pass filtered at 200 Hz. Prior to the experiment, we explained the experimental paradigm and procedures to participants and their parents. Participants practiced one block of the motor task to familiarize themselves with the experimental environment and paradigm. Participants were recorded in a comfortable supine position on a bed during MEG measurement, and two experimenters stayed beside the participants to support them to maintain their attention on the task.

Four head positioning coils were attached to the scalp (Cz, 5 cm anterior from Cz, and 5 cm from the superior side of the left and right pre-auricular points). The location of the positioning coils was measured before MEG recording to calculate the position of the participant's head relative to the MEG sensors. The participants were carefully monitored using a video monitoring system to assess their compliance with the instructions and to record any notable artifacts, such as head motion, inappropriate head position, or inconsistent attention to the screen. The location of the positioning coils and information about head-shape were measured using a 3D digitizer (Fastrak, Polhemus, Colchester, VT, USA).

Brain structural images were individually obtained for source reconstruction from all participants using a 1.5 Tesla magnetic resonance imaging (MRI) scanner (SIGNA Explorer, GE Healthcare, USA). For each participant, an MRI scan was acquired using a T1-weighted gradient echo and Silenz pulse sequence (repetition time [TR] = 435.68 ms, echo time [TE] = 0.024 ms, flip angle = 7°, field of view [FOV] = 220 mm, matrix size = 256 × 256 pixels, slice thickness = 1.7 mm, and 130 transaxial images).

2.4. Data analysis

MEG data were processed using the Brainstorm toolbox (Tadel et al., 2011) and MATLAB (Mathworks, Natick, MA, USA). Data were band-pass filtered from 0.3 to 200 Hz and notch filtered at 60, 120, and 180 Hz. We applied an independent component analysis method ("RunICA" implemented in Brainstorm, www.sccn.ucsd.edu/eeglab/) and removed the components representing heartbeats, eye blinks, and eye movements identified by visual inspection based on time course and topography. The number of rejected components per participant did not differ between the TD and ASD groups (TD: mean = 1.89, SD = 0.81; ASD: mean = 2.22, SD = 0.88; p = 0.25). After rejecting the components representing artifacts, the remaining components were back-projected into the signal space. We epoched data into segments from − 3 to 3 s following button-press onset and selected successful trials.

We calculated weighted minimum norm estimates (wMNE)

implemented in the Brainstorm toolbox for source analysis (Hämäläinen and Ilmoniemi, 1994; Hauk, 2004; Lin et al., 2006). We estimated an overlapping sphere head model using individual MRI images and the noise-covariance matrix using the baseline period (−2 to − 1.5 s). We applied wMNE source localization using an overlapping conductor model with a Tikhonov regularization factor (λ = 0.1).

We calculated movement-related fields (MRFs) by averaging all trials according to the button-press onset and normalizing by the baseline period (−2 to −1.5 s) for each participant. We computed the cortical sources of the individual MRFs at 20 to 40 ms and found the maximum peak source in the bilateral cortex of each participant. These individual cortical sources were projected on the ICBM152 template anatomy in MNE coordinates (Table 2). We observed that these cortical sources were in the bilateral M1 and used these cortical sources for further oscillatory analysis (Fig. 2A).

To determine the motor-related oscillatory changes, single-trial source data were used to calculate the time–frequency representations (TFRs) using a seven-cycle Morlet wavelet. We converted TFRs to the percentage change in power relative to the baseline period. TFRs of each trial source were averaged within participants and group-averaged across TD participants and participants with ASD, respectively. To define statistically significant motor-related gamma oscillations and pre-movement beta oscillations, we applied one-sample t-tests on the full TFRs from all participants with the false discovery rate (FDR) correction to correct for multiple comparisons. We observed a significant increase in gamma oscillations from 70 to 90 Hz during 0 to 100 ms, according to button responses. We calculated the power change by averaging power values in these time and frequency window and defined it as a movement-related gamma increase. We observed a significant decrease in beta oscillations from 15 to 25 Hz during −200 to 500 ms, according to button responses. We defined beta decrease during −200 to 0 ms as a pre-movement beta decrease and those during 0 to 500 ms as a movement-related beta decrease. We calculated the power changes of the pre-movement beta decrease and movement-related beta decrease by averaging power values in these time and frequency windows.

To estimate the phase-amplitude coupling between the beta and gamma oscillations, we used Mean Vector Length analysis implemented in the Brainstorm toolbox (Canolty et al., 2006; Tort et al., 2010). To calculate PAC, the data length containing 10 cycles of the lowest frequency is required. Thus, we selected a 1-s time window from − 200 ms, which is the start of the pre-movement beta decrease, until 800 ms. This time window covered motor-related gamma increases and pre-movement beta decreases. We calculated PAC between the phase at 13

Table 2

Individual button response time and bilateral source locations of motor-related fields at 20–40 ms.

Participant	Button response time (ms)		Left cortical source of motor-related fields (20–40 ms, MNI coordinates)				Right cortical source of motor-related fields (20–40 ms, MNI coordinates)		
	mean	median	X	Y	Z		X	Y	Z
TD children									
TD01	542.7	494.5	−42.1	1.4	55.1		61.8	11.5	41.8
TD02	434.0	372.5	−25.5	−16.2	65.0		28.8	−1.4	61.8
TD03	445.2	415.2	−39.1	−2.4	62.4		19.9	−16.3	70.2
TD04	643.4	554.8	−41.9	0.8	51.3		48.0	3.2	51.4
TD05	397.5	359.1	−44.5	−5.6	50.5		42.9	−8.7	38.0
TD06	464.2	471.4	−49.4	−3.4	54.0		42.2	2.6	53.3
TD07	379.8	335.0	−37.3	−5.2	58.6		60.1	−0.4	29.5
TD08	406.1	342.7	−45.7	−0.0	60.2		58.8	−6.5	33.7
TD09	450.1	427.0	−34.2	−2.7	60.2		48.8	−6.4	50.1
TD10	378.9	349.0	−24.6	−11.9	70.5		37.6	−8.1	62.1
TD11	333.8	320.5	−48.3	8.3	53.8		51.7	23.4	49.8
TD12	362.6	306.0	−21.7	−11.3	68.4		38.8	−12.9	64.6
TD13	555.1	515.7	−28.8	−8.1	67.2		46.1	−11.3	55.2
TD14	493.5	465.5	−39.7	−0.9	63.9		58.2	−3.9	45.5
TD15	293.8	270.0	−45.6	3.4	56.5		51.8	−8.1	45.1
TD16	693.4	568.5	−47.5	0.7	51.8		40.2	1.3	67.6
TD17	341.5	310.2	−46.4	−1.5	56.4		40.6	−12.6	49.9
TD18	419.1	394.0	−42.9	−5.7	54.5		45.7	10.8	46.5
TD19	382.1	364.0	−40.8	0.5	59.4		58.7	−8.2	49.3
Mean	*442.99*	*401.87*	*−39.3*	*−3.1*	*58.9*		*46.4*	*−2.7*	*50.8*
SD	*104.16*	*87.86*	*8.5*	*5.8*	*5.9*		*11.0*	*9.9*	*11.1*
Children with ASD									
ASD01	519.6	477.2	−47.1	9.7	49.2		43.0	−11.8	56.5
ASD02	742.5	635.0	−39.4	−1.1	61.2		54.4	−0.7	41.2
ASD03	714.0	653.5	−37.5	−2.3	59.4		52.6	7.2	42.7
ASD04	427.1	393.8	−34.6	−11.5	74.2		36.5	−14.0	73.0
ASD05	495.8	403.9	−37.4	−16.2	61.3		45.2	−2.5	52.0
ASD06	962.2	892.9	−44.1	−15.8	49.3		46.2	−6.0	52.8
ASD07	540.4	485.8	−46.6	−5.3	2.7		36.4	−31.4	15.7
ASD08	670.8	573.3	−47.1	4.0	44.3		53.4	−5.2	49.1
ASD09	724.5	621.5	−39.3	−11.0	52.6		30.7	−3.7	56.5
ASD10	490.7	445.0	−44.6	−14.1	63.2		46.7	3.0	60.0
ASD11	398.1	365.0	−55.1	0.1	44.7		36.4	5.9	48.4
ASD12	614.6	525.5	−57.6	−11.8	53.1		48.6	9.7	45.9
ASD13	599.3	546.5	−27.0	−6.0	69.0		39.9	−13.4	49.6
ASD14	839.1	740.5	−43.6	−5.1	52.4		51.3	−0.7	50.6
ASD15	639.6	561.0	−51.9	−4.5	39.3		36.7	−12.3	60.6
ASD16	300.0	278.0	−55.8	−3.2	48.0		47.2	−9.3	56.5
ASD17	524.9	493.8	−47.4	2.5	52.3		61.2	7.8	39.7
ASD18	628.0	522.0	−48.3	11.4	11.5		53.7	25.3	10.2
Mean	*601.73*	*534.12*	*−44.3*	*−5.9*	*51.5*		*44.1*	*−5.3*	*50.7*
SD	*161.57*	*143.90*	*8.3*	*7.2*	*16.1*		*7.2*	*10.2*	*12.1*

to 30 Hz and amplitude at 30 to 200 Hz in the time window during motor control (−200 to 800 ms). The statistical dependence of modulation of the gamma band activity by the beta rhythm was calculated as the modulation index. To define statistically obvious motor-related PAC signals, we applied one-sample t-tests for the full PAC maps from all participants with FDR correction to correct for multiple comparisons. In the PAC maps, we selected obvious PAC signals between 13 Hz and 100 to 140 Hz, and averaged across modulation indices in this window.

We used power changes of motor-related gamma oscillations and pre-movement beta oscillations as well as beta-gamma coupling in the bilateral M1 for further statistical analysis.

2.5. Statistical analysis

We used SPSS version 24.0 (IBM Corporation, New York, USA) for statistical analysis. We applied two-sample t-tests (two-tailed) to compare differences in participant characteristics (age, K-ABC scores) between the TD and ASD groups. For button response time, we applied a Welch t-test (two-tailed) to consider their unequal variance between two groups. To test our hypothesis, we compared power changes in motor-related gamma and pre-movement and movement-realted beta oscillations and beta-gamma coupling between two groups using two-sample t-tests (two-tailed). We calculated Pearson's correlation coefficients to

test the correlations between response time and the significant neurophysiological indices. To take into account its effect on the significant indices, response time was included as a nuisance covariate in the analysis of covariance (ANCOVAs). We employed an alpha level of 0.05 for all statistical analyses.

To investigate the ability of both behavioral and neural indices to classify participants into TD and ASD groups, we performed Fisher's linear discriminant analysis with the leave-one-out cross-validation test. To test the predictive accuracy of the classification method, we employed behavioral and brain oscillatory indices representing significant differences between group. For the cross-validation test, each case was excluded from all other cases, and the remaining cases were classified. We analyzed the receiver operator characteristic (ROC) curves using sensitivity and 1 − specificity from the results of linear discriminant analysis. Participants' discriminative capacity was determined by the area under the ROC curve (AUC).

3. Results

3.1. Button response time

We selected trials in which participants pressed the button within 200 to 2000 ms after the visual target onset to exclude failed and
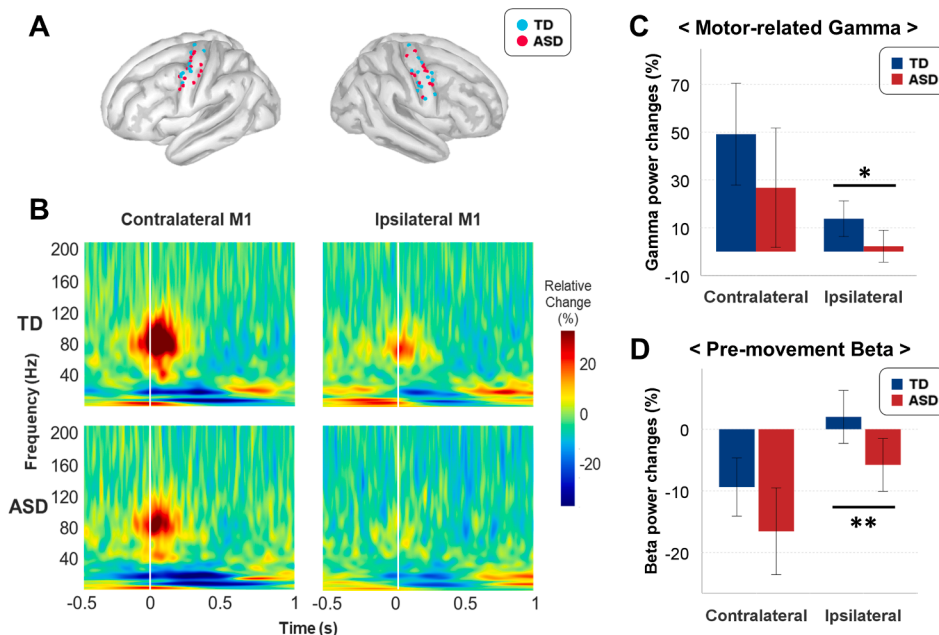
Fig. 2. Motor-related oscillatory changes in the TD and ASD groups. **A.** Individual peak source of motor-related brain activity. Red dots indicate the source for children with ASD and blue dots indicate the source for TD children. **B.** Time-frequency representations during motor control in the bilateral primary motor cortex (M1) in the TD and ASD groups. Motor-related gamma oscillations (70 to 90 Hz) increased immediately after the button press. The pre-movement beta oscillations (15 to 25 Hz) decreased 200 ms prior to the button press. **C.** Motor-related gamma increases were calculated by averaging across the window between 70 and 90 Hz and 0 to 100 ms. The vertical error bars represent the 95% confidence interval for each of the bars. The ASD group exhibited a smaller gamma power increase than the TD group in the ipsilateral M1, but not in the contralateral M1. **D.** Pre-movement beta decreases were calculated by averaging across the window between 15 and 25 Hz and −200 to 0 ms. The vertical error bars represent the 95% confidence interval for each of the bars. The ASD group showed enhanced pre-movement beta decreases in ipsilateral M1, but not in contralateral M1. (For interpretation of the references to colour in this figure legend, the reader is referred to the web version of this article.)

accidental button responses. The button response time was considered as the latency between the visual trigger and button-press onset (Table 2). For the individual button response time, we used the mean of the button response time within each subject. The mean response time of the TD group was 443.0 ± 104.2 ms (mean ± SD), and that of the ASD group was 601.7 ± 161.6 ms (mean ± SD). Consistent with our previous study, the ASD group exhibited a significantly longer mean response time than the TD group ($t(28.804) = −3.531, p = 0.001$, Cohen's $d = −1.175$) (Fig. 1B).

3.2. Motor-related oscillatory changes

Fig. 2B shows the group-averaged time–frequency representations from the individual bilateral peak source of motor fields in 19 TD children and 18 children with ASD. Gamma oscillatory power increased in the 70 to 90 Hz range immediately after the button press onset. The decrease of beta oscillatory power in the 15 to 25 Hz range started approximately 200 ms prior to the button press onset.

We observed diminished gamma power increase in the ASD group compared with the TD group in ipsilateral M1 ($t(35) = 2.412, p = 0.021$, Cohen's $d = 0.793$), but not in contralateral M1 ($t(35) = 1.442, p = 0.158$, Cohen's $d = 0.474$) (Fig. 2C). The pre-movement beta power decrease was significantly enhanced in the ASD group compared with the TD group in ipsilateral M1 ($t(35) = 2.705, p = 0.010$, Cohen's $d = 0.890$), but not contralateral M1 ($t(35) = 1.804, p = 0.08$, Cohen's $d = 0.593$) (Fig. 2D). In contrast, we could not find any differences in the movement-related beta power decrease between TD and ASD group in the contralateral ($t(35) = 1.126, p = 0.268$, Cohen's $d = 0.370$) and ipsilateral cortex ($t(35) = -0.008, p = 0.993$, Cohen's $d = -0.003$). The ipsilateral motor-related gamma increase and pre-movement beta decrease had no correlations with response time within TD group ($r = −0.009, p = 0.970$ for gamma, $r = −0.147, p = 0.547$ for beta), ASD group ($r = 0.251, p = 0.314$ for gamma, $r = −0.126, p = 0.617$ for beta), and all participants ($r = −0.091, p = 0.593$ for gamma, $r = −0.317, p = 0.056$ for beta). The ANCOVA analysis with a response time as a covariate showed a significant group effect on the ipsilateral motor-related gamma increase ($F = 6.017, p = 0.019$), but not on the ipsilateral pre-movement beta decrease ($F = 3.621, p = 0.066$).

3.3. Motor-related phase-amplitude coupling

We calculated the phase-amplitude coupling between beta (13 to 30 Hz) and gamma (40 to 200 Hz) frequency ranges. We found PAC signals between beta (13 Hz) and high-gamma oscillations (100 to 140 Hz) in bilateral M1 in the TD and ASD groups (Fig. 3A).

The ASD group exhibited significantly lower PAC signals than the TD group for ipsilateral M1 ($t(35) = 3.610, p = 0.001$, Cohen's $d = 1.187$), but not contralateral M1 ($t(35) = 0.599, p = 0.553$, Cohen's $d = 0.197$) (Fig. 3B). The ipsilateral PAC signal had no correlations with response time within TD group ($r = −0.059, p = 0.811$), ASD group ($r = −0.004, p = 0.987$), and all participants ($r = −0.287, p = 0.085$). The ANCOVA analysis with a response time as a covariate showed significantly reduced ipsilateral PAC signal ($F = 8.835, p = 0.005$) in the ASD group.

3.4. Classification using linear discriminant analysis

We found significant differences in button response time, ipsilateral motor-related gamma increase, pre-movement beta decrease, and beta-gamma PAC between TD and ASD groups. To investigate the efficiency of the classifier for distinguishing between the two groups, we conducted linear discriminant analysis using these variables. Using response time and ipsilateral motor-related gamma increase, a linear discriminant analysis classifier identified participants into two groups with 67.6% accuracy (66.7% sensitivity and 68.4% specificity), and its ROC curve showed AUC of 0.863 (Supplementary Fig. 1A). Using response time and ipsilateral pre-movement beta decrease, a linear discriminant analysis classifier showed 78.4% accuracy (77.8% sensitivity and 78.9% specificity), and its ROC curve showed AUC of 0.845 (Supplementary Fig. 1B). Using response time and ipsilateral beta-gamma PAC, a linear discriminant analysis classifier showed 81.1% accuracy (77.8% sensitivity and 84.2% specificity), and its ROC curve showed AUC of 0.880 (Supplementary Fig. 1C). Using response time, ipsilateral pre-movement beta decrease, and beta-gamma PAC, a linear discriminant analysis classifier showed 81.1% accuracy (77.8% sensitivity and 84.2% specificity), and its ROC curve showed AUC of 0.892 (Supplementary Fig. 1D). Using response time, ipsilateral motor-related gamma increase, and beta-gamma PAC, a linear discriminant analysis classifier showed 83.8% accuracy (77.8% sensitivity and 89.5% specificity) (Fig. 4A), and
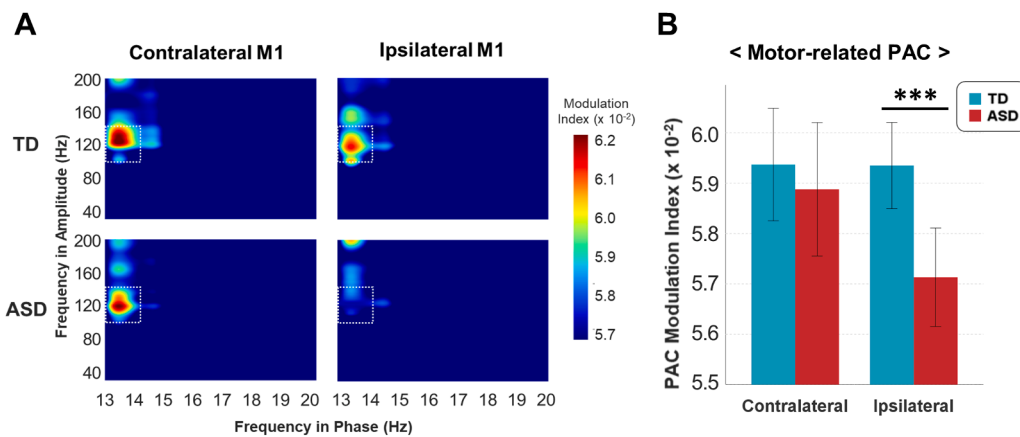
Fig. 3. Phase amplitude coupling (PAC) in bilateral primary motor cortex (M1). **A.** During motor control, PAC between the low beta (approximately 13 Hz) and high-gamma oscillations (100 to 140 Hz) was observed in bilateral M1. **B.** Beta-gamma PAC was calculated by averaging across the window between beta (13 Hz) and high-gamma (100 to 140 Hz). The vertical error bars represent the 95% confidence interval for each of the bars. The modulation index of PAC in contralateral M1 was not different between the two groups. The ASD group exhibited significantly reduced beta-gamma PAC in ipsilateral M1 compared with the TD group.
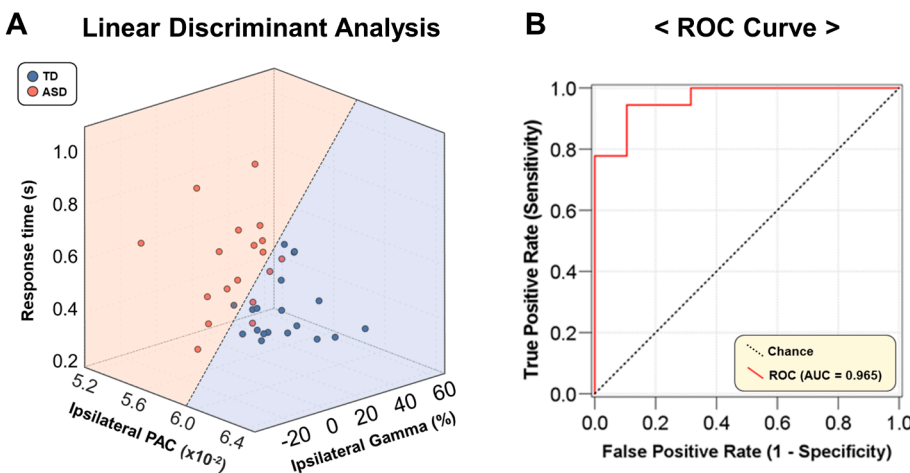

Fig. 4. Linear discriminant analysis and receiver operating characteristic (ROC) curve using oscillations and oscillatory coupling parameters. **A.** The linear discriminant analysis used response time, ipsilateral gamma and beta-gamma PAC. The discriminant classifier results exhibited accuracy of 83.8% (sensitivity = 77.8%, specificity = 89.5%) for blindly separating the two groups. **B.** Using these indices, the ROC curve exhibited a good discriminative capacity for the two groups with an area under the ROC curve (AUC) value of 0.965.

its ROC curve showed AUC of 0.965 (Fig. 4B, Supplementary Fig. 1E). Using response time, ipsilateral pre-movement beta decrease, motor-related gamma increase, and beta-gamma PAC, a linear discriminant analysis showed 86.5% accuracy (83.3% sensitivity and 89.5% specificity), and its ROC curve showed AUC of 0.956 (Supplementary Fig. 1F).

4. Discussion

Using MEG, we examined oscillatory changes and oscillatory coupling in M1 to investigate the neural mechanisms underlying motor dysfunction in ASD. We confirmed prolonged response times during the motor task in the ASD group compared with the TD group. In addition, we observed alterations in motor-related gamma oscillations and pre-movement beta oscillations in the ASD group. Oscillatory coupling, by which the beta rhythm modulated high-gamma activity, was reduced in the ASD group. In addition, using motor behavior and motor-related oscillatory changes and oscillatory coupling, we identified a potential biomarker for ASD.

4.1. Button response time

We confirmed that the button response time in the ASD group was prolonged by approximately 150 ms compared with the TD group. The finding of an increased response time is in accord with previous behavioral studies. Numerous previous studies have reported that individuals with ASD exhibit broad motor deficits in gross and fine motor skills, posture, gait, and balance (Teitelbaum et al., 1998; Noterdaeme et al., 2002; Molloy et al., 2003; Jansiewicz et al., 2006; Bryson et al.,

2007; Fournier et al., 2010; Lloyd et al., 2013; Radonovich et al., 2013). The prolonged button response time of children with ASD might be related to their motor dysfunction.

4.2. Motor-related oscillatory changes

We observed motor-related gamma increases and pre-movement and movement-related beta decreases in bilateral M1 of TD and ASD groups. The results revealed that the ASD group exhibited alterations in the motor-related gamma increase and pre-movement beta decrease in M1.

We confirmed that motor-related gamma oscillations were reduced in participants with ASD, consistent with our previous findings (An et al., 2018). The power of gamma oscillations is reported to be increased immediately after movement onset in adults (Cheyne et al., 2008; Muthukumaraswamy, 2010) and children (Gaetz et al., 2010; Cheyne et al., 2014). This transient gamma increase is thought to be related to the initiation of movement and motor execution (Cheyne et al., 2008; Muthukumaraswamy, 2010; Cheyne and Ferrari, 2013). In the present study, the results indicated that altered motor-related gamma activity reflected impaired movement initiation in ASD.

In addition, we found that the finger movement suppressed the power of pre-movement and movement-related beta oscillations in both groups. Adult participants exhibited a pre-movement beta power decrease approximately 2 to 1 s prior to movement onset during self-paced movement (Stancák and Pfurtscheller, 1996; Pfurtscheller and Lopes da Silva, 1999; Pfurtscheller et al., 2003; Bai et al., 2011) and pre-cued motor tasks (Kaiser et al., 2001; Doyle et al., 2005; Gaetz et al., 2010). In the current study, children showed a pre-movement beta

decrease starting approximately 200 ms prior to movement onset. This late latency of pre-movement beta decreases is consistent with the results of previous MEG studies in children (Cheyne et al., 2014). Pre-movement beta decreases are thought to be related to movement planning and movement preparation for appropriate motor responses (Stancák and Pfurtscheller, 1996; Kaiser et al., 2001; Doyle et al., 2005). We observed that the ASD group showed a significant enhancement in the beta decreases before movement onset (i.e. pre-movement beta decreases), not in the beta decreases after movement onset (i.e. movement-related beta decreases). The enhanced pre-movement beta decreases in the ASD group might reflect a requirement for stronger brain activity compared with the TD group to compensate for deficits during movement planning and movement preparation.

4.3. Motor-related phase-amplitude coupling

In the current MEG study, the results revealed oscillatory coupling, by which high gamma brain activity at 100 to 140 Hz was modulated by the beta rhythm at 13 Hz in M1 in children. The frequency range of the oscillatory coupling was different from the frequency band of beta power changes (i.e., 15 to 25 Hz) and gamma power changes (i.e., 70 to 90 Hz). The different frequency ranges between oscillatory power changes and oscillatory coupling might reflect their mechanisms and indirect relationships.

The beta-high gamma coupling measured by MEG in the present study is consistent with PAC patterns revealed using invasive local field potential measurement techniques. Previous ECoG studies reported coupling between the amplitude of high-gamma activity and the phase of the beta rhythm in human M1 (de Hemptinne et al., 2013, 2015). Cross-frequency coupling has also been observed between the gamma activity from M1 and the low-frequency oscillations from the ventral intermediate nucleus (i.e., the motor nucleus of the thalamus) (Opri et al., 2019). Thalamo-cortical PAC has been suggested to act as a mechanism for gating motor behavior. Therefore, our finding that the slow rhythm modulates fast brain activity in M1 might reflect an underlying gating mechanism for motor execution, and could be related to distal communication mediated by the thalamus across the thalamo-cortical motor network.

It has been suggested that high-frequency brain activity, such as gamma oscillation, is related to local cortical processing over relatively short spatial scales (Jensen and Colgin, 2007; Miller et al., 2007, 2009) and is correlated with blood-oxygen-level-dependent signals (Mukamel et al., 2005; Niessing et al., 2005; Scheeringa et al., 2011). In contrast, given conduction delays, low-frequency oscillations are thought to transfer information over large spatial scales by coordinating activities in distinct cortical areas (von Stein and Sarnthein, 2000; Buzsaki, 2004; Canolty et al., 2006; Jensen and Colgin, 2007; Canolty and Knight, 2010). Therefore, the coupling between slow- and fast-frequency oscillations has been proposed as a mechanism for local connectivity by coordinating activity in distributed brain regions across multiple spatial and temporal scales (Canolty et al., 2006; Jensen and Colgin, 2007; Canolty and Knight, 2010).

In the present study, we found that beta-high gamma coupling was reduced in M1 in the ASD group. These findings are consistent with previous studies reporting that individuals with ASD exhibit reduced PAC during visual gating tasks (Seymour et al., 2019) and face recognition tasks (Khan et al., 2013; Mamashli et al., 2018). Previous studies have proposed that aberrant PAC in ASD is linked to dysregulation of local connectivity and sensory processing. The current findings suggest that reduced PAC in M1 might reflect atypical local brain connectivity and dysregulated motor processing in ASD.

In addition, we investigated potential biomarkers for ASD using behavioral and neurophysiological oscillatory indices, revealing that linear discriminant analysis was able to classify these two groups. Although ASD involves various symptoms, we found that brain oscillations and oscillatory coupling during motor control discriminated between participants with ASD and TD participants with high accuracy. Although ASD is assumed to involve a range of pathophysiological mechanisms, the current finding that motor-related indices were able to discriminate between individuals with ASD and TD controls with high accuracy suggests that motor dysfunction is a common and important component of ASD. These findings support the notion that motor dysfunction in ASD should be considered as an important characteristic of ASD.

5. Study limitations

Our study involved several major limitations that should be considered. First, because the current findings were obtained from a relatively small number of participants, the results are not sufficient for drawing firm conclusions about biomarkers for ASD. Future studies should examine a larger sample size and age range of participants to improve the reliability of the findings. Second, we calculated the mean of the button-response times within each subject to see the tendency of their response time and their consistency with our previous study. The means might tend to be biased due to a few long response times in the distribution. Last, we recorded the head movement of the children participants using video monitors rather than using a simultaneous head positioning system during the MEG recordings. When participants exhibited substantial head movement, the corresponding MEG signals were eliminated from the analysis by visual inspection. Further investigations should use a quantification algorithm for head movement to increase the reliability of the data.

6. Conclusions

Coupling between distinct oscillations in M1 has previously only been observed using local field potentials measured with invasive ECoG recording. In the present study, we demonstrated that the beta rhythm modulated high-gamma activity in M1 using non-invasive MEG recording. In addition, the current results revealed that beta-high gamma coupling was reduced in the ASD group. This finding extends current understanding of motor gating dysfunction in ASD. We confirmed aberrant motor-related gamma activity and found enhanced pre-movement beta power during motor control in individuals with ASD. These findings provide neurophysiological evidence for dysfunction of motor initiation and motor preparation in ASD. In addition, these findings could be applied in future studies examining interventions or neurofeedback training for ASD.

CRediT authorship contribution statement

Kyung-min An: Conceptualization, Data curation, Formal analysis, Investigation, Methodology, Visualization, Writing - original draft, Writing - review & editing. **Takashi Ikeda:** Data curation, Software, Methodology, Writing - review & editing. **Chiaki Hasegawa:** Data curation, Writing - review & editing. **Yuko Yoshimura:** Data curation, Writing - review & editing. **Sanae Tanaka:** Data curation, Writing - review & editing. **Daisuke N. Saito:** Data curation, Writing - review & editing. **Ken Yaoi:** Data curation, Writing - review & editing. **Sumie Iwasaki:** Data curation, Writing - review & editing. **Tetsu Hirosawa:** Methodology, Writing - review & editing. **Ole Jensen:** Methodology, Investigation, Supervision, Writing - review & editing. **Mitsuru Kikuchi:** Conceptualization, Writing - review & editing, Supervision, Funding acquisition, Project administration.

Declaration of Competing Interest

The authors declare that they have no known competing financial interests or personal relationships that could have appeared to influence the work reported in this paper.

Appendix A. Supplementary data

Supplementary data to this article can be found online at https://doi.org/10.1016/j.nicl.2021.102560.

References

An, K.-M., Ikeda, T., Yoshimura, Y., Hasegawa, C., Saito, D.N., Kumazaki, H., Hirosawa, T., Minabe, Y., Kikuchi, M., 2018. Altered gamma oscillations during motor control in children with autism spectrum disorder. J. Neurosci. 38 (36), 7878–7886.

American Psychiatric Association, 2013. American Psychiatric Association: Diagnostic and Statistical Manual of Mental Disorders (DSM-5®). American Psychiatric Association.

Bai, O.u., Rathi, V., Lin, P., Huang, D., Battapady, H., Fei, D.-Y., Schneider, L., Houdayer, E., Chen, X., Hallett, M., 2011. Prediction of human voluntary movement before it occurs. Clin. Neurophysiol. 122 (2), 364–372.

Bryson, S.E., Zwaigenbaum, L., Brian, J., Roberts, W., Szatmari, P., Rombough, V., McDermott, C., 2007. A Prospective Case Series of High-risk Infants who Developed Autism. J Autism Dev Disord 37 (1), 12–24.

Buzsaki, G., 2004. Neuronal Oscillations in Cortical Networks. Science 304 (5679), 1926–1929.

Canolty, R.T., Edwards, E., Dalal, S.S., Soltani, M., Nagarajan, S.S., Kirsch, H.E., Berger, M.S., Barbaro, N.M., Knight, R.T., 2006. High Gamma Power Is Phase-Locked to Theta Oscillations in Human Neocortex. Science 313 (5793), 1626–1628.

Canolty, R.T., Knight, R.T., 2010. The functional role of cross-frequency coupling. Trends Cognitive Sci. 14 (11), 506–515.

Cheyne, D., Bells, S., Ferrari, P., Gaetz, W., Bostan, A.C., 2008. Self-paced movements induce high-frequency gamma oscillations in primary motor cortex. NeuroImage 42 (1), 332–342.

Cheyne, D., Ferrari, P., 2013. MEG studies of motor cortex gamma oscillations: evidence for a gamma "fingerprint" in the brain? Front. Hum. Neurosci. 7, 575.

Cheyne, D., Jobst, C., Tesan, G., Crain, S., Johnson, B., 2014. Movement-related neuromagnetic fields in preschool age children: Movement-Related Brain Activity in Preschool Children. Hum. Brain Mapp. 35 (9), 4858–4875.

de Hemptinne, C., Ryapolova-Webb, E.S., Air, E.L., Garcia, P.A., Miller, K.J., Ojemann, J. G., Ostrem, J.L., Galifianakis, N.B., Starr, P.A., 2013. Exaggerated phase-amplitude coupling in the primary motor cortex in Parkinson disease. Proc. Natl. Acad. Sci. 110 (12), 4780–4785.

de Hemptinne, C., Swann, N.C., Ostrem, J.L., Ryapolova-Webb, E.S., San Luciano, M., Galifianakis, N.B., Starr, P.A., 2015. Therapeutic deep brain stimulation reduces cortical phase-amplitude coupling in Parkinson's disease. Nat. Neurosci. 18 (5), 779–786.

Doyle, L.M.F., Yarrow, K., Brown, P., 2005. Lateralization of event-related beta desynchronization in the EEG during pre-cued reaction time tasks. Clin. Neurophysiol. 116 (8), 1879–1888.

Fournier, K.A., Hass, C.J., Naik, S.K., Lodha, N., Cauraugh, J.H., 2010. Motor Coordination in Autism Spectrum Disorders: A Synthesis and Meta-Analysis. J. Autism Dev. Disord. 40 (10), 1227–1240.

Gaetz, W., MacDonald, M., Cheyne, D., Snead, O.C., 2010. Neuromagnetic imaging of movement-related cortical oscillations in children and adults: Age predicts post-movement beta rebound. NeuroImage 51 (2), 792–807.

Hämäläinen, M.S., Ilmoniemi, R.J., 1994. Interpreting magnetic fields of the brain: minimum norm estimates. Med. Biol. Eng. Comput. 32 (1), 35–42.

Hauk, O., 2004. Keep it simple: a case for using classical minimum norm estimation in the analysis of EEG and MEG data. NeuroImage 21 (4), 1612–1621.

Hyafil, A., Giraud, A.-L., Fontolan, L., Gutkin, B., 2015. Neural Cross-Frequency Coupling: Connecting Architectures, Mechanisms, and Functions. Trends Neurosci. 38 (11), 725–740.

Jansiewicz, E.M., Goldberg, M.C., Newschaffer, C.J., Denckla, M.B., Landa, R., Mostofsky, S.H., 2006. Motor Signs Distinguish Children with High Functioning Autism and Asperger's Syndrome from Controls. J. Autism Dev. Disord. 36 (5), 613–621.

Jensen, O., Colgin, L.L., 2007. Cross-frequency coupling between neuronal oscillations. Trends Cognitive Sci. 11 (7), 267–269.

Kaiser, J., Birbaumer, N., Lutzenberger, W., 2001. Event-related beta desynchronization indicates timing of response selection in a delayed-response paradigm in humans. Neurosci. Lett. 312 (3), 149–152.

Kanner, L., 1943. Autistic disturbances of affective contact. Nervous Child. 2, 217–250.

Khan, S., Gramfort, A., Shetty, N.R., Kitzbichler, M.G., Ganesan, S., Moran, J.M., Lee, S. M., Gabrieli, J.D.E., Tager-Flusberg, H.B., Joseph, R.M., Herbert, M.R., Hamalainen, M.S., Kenet, T., 2013. Local and long-range functional connectivity is reduced in concert in autism spectrum disorders. Proc. Natl. Acad. Sci. 110 (8), 3107–3112.

Lin, F.-H., Witzel, T., Ahlfors, S.P., Stufflebeam, S.M., Belliveau, J.W., Hämäläinen, M.S., 2006. Assessing and improving the spatial accuracy in MEG source localization by depth-weighted minimum-norm estimates. NeuroImage 31 (1), 160–171.

Lloyd, M., MacDonald, M., Lord, C., 2013. Motor skills of toddlers with autism spectrum disorders. Autism 17 (2), 133–146.

London, E.B., 2014. Categorical diagnosis: a fatal flaw for autism research? Trends Neurosci. 37, 683–686.

Lord, C., Risi, S., Lambrecht, L., Cook Jr., E.H., Leventhal, B.L., DiLavore, P.C., Pickles, A., Rutter, M., 2000. The autism diagnostic observation schedule-generic: a standard measure of social and communication deficits associated with the spectrum of autism. J. Autism Dev. Disord. 30, 205–223.

Mamashli, F., Khan, S., Bharadwaj, H., Losh, A., Pawlyszyn, S.M., Hämäläinen, M.S., Kenet, T., 2018. Maturational trajectories of local and long-range functional connectivity in autism during face processing. Hum. Brain Mapp. 39 (10), 4094–4104.

Miller, K.J., Leuthardt, E.C., Schalk, G., Rao, R.P.N., Anderson, N.R., Moran, D.W., Miller, J.W., Ojemann, J.G., 2007. Spectral Changes in Cortical Surface Potentials during Motor Movement. J. Neurosci. 27 (9), 2424–2432.

Miller, K.J., Zanos, S., Fetz, E.E., den Nijs, M., Ojemann, J.G., 2009. Decoupling the Cortical Power Spectrum Reveals Real-Time Representation of Individual Finger Movements in Humans. J. Neurosci. 29 (10), 3132–3137.

Molloy, C.A., Dietrich, K.N., Bhattacharya, A., 2003. Postural Stability in Children with Autism Spectrum Disorder. J. Autism Dev. Disord. 33 (6), 643–652.

Mukamel, R., Gelbard, H., Arieli, A., Hasson, U., Fried, I., Malach, R., 2005. Coupling between neuronal firing, field potentials, and FMRI in human auditory cortex. Science 309, 951–954.

Muthukumaraswamy, S.D., 2010. Functional Properties of Human Primary Motor Cortex Gamma Oscillations. J. Neurophysiol. 104 (5), 2873–2885.

Niessing, J., Ebisch, B., Schmidt, K.E., Niessing, M., Singer, W., Galuske, R.A., 2005. Hemodynamic signals correlate tightly with synchronized gamma oscillations. Science 309, 948–951.

Noterdaeme, M., Mildenberger, K., Minow, F., Amorosa, H., 2002. Evaluation of neuromotor deficits in children with autism and children with a specific speech and language disorder. Eur. Child Adolesc. Psychiatry. 11, 219–225.

Oldfield, R.C., 1971. The assessment and analysis of handedness: The Edinburgh inventory. Neuropsychologia 9 (1), 97–113.

Opri, E., Cernera, S., Okun, M.S., Foote, K.D., Gunduz, A., 2019. The Functional Role of Thalamocortical Coupling in the Human Motor Network. J. Neurosci. 39 (41), 8124–8134.

Pfurtscheller, G., Graimann, B., Huggins, J.E., Levine, S.P., Schuh, L.A., 2003. Spatiotemporal patterns of beta desynchronization and gamma synchronization in corticographic data during self-paced movement. Clin. Neurophysiol. 114 (7), 1226–1236.

Pfurtscheller, G., Lopes da Silva, F.H., 1999. Event-related EEG/MEG synchronization and desynchronization: basic principles. Clin. Neurophysiol. 110 (11), 1842–1857.

Radonovich, K.J., Fournier, K.A., Hass, C.J., 2013. Relationship between postural control and restricted, repetitive behaviors in autism spectrum disorders. Front. Integr. Neurosci. 7, 28.

Scheeringa, R., Fries, P., Petersson, K.-M., Oostenveld, R., Grothe, I., Norris, D.G., Hagoort, P., Bastiaansen, M.C.M., 2011. Neuronal Dynamics Underlying High- and Low-Frequency EEG Oscillations Contribute Independently to the Human BOLD Signal. Neuron 69 (3), 572–583.

Seymour, R.A., Rippon, G., Gooding-Williams, G., Schoffelen, J.M., Kessler, K., 2019. Dysregulated oscillatory connectivity in the visual system in autism spectrum disorder. Brain. 142, 3294-3305.

Stancák Jr., A., Pfurtscheller, G., 1996. Event-related desynchronisation of central beta-rhythms during brisk and slow self-paced finger movements of dominant and nondominant hand. Cognitive Brain Res. 4 (3), 171–183.

Tadel, F., Baillet, S., Mosher, J.C., Pantazis, D., Leahy, R.M., 2011. Brainstorm: A User-Friendly Application for MEG/EEG Analysis. Computational Intelligence Neurosci. 2011, 1–13.

Teitelbaum, P., Teitelbaum, O., Nye, J., Fryman, J., Maurer, R.G., 1998. Movement analysis in infancy may be useful for early diagnosis of autism. Proc. Natl. Acad. Sci. 95 (23), 13982–13987.

Tort, A.B.L., Komorowski, R., Eichenbaum, H., Kopell, N., 2010. Measuring Phase-Amplitude Coupling Between Neuronal Oscillations of Different Frequencies. J. Neurophysiol. 104 (2), 1195–1210.

von Stein, A., Sarnthein, J., 2000. Different frequencies for different scales of cortical integration: from local gamma to long range alpha/theta synchronization. Int. J. Psychophysiol. 38 (3), 301–313.

Wing, L., Leekam, S.R., Libby, S.J., Gould, J., Larcombe, M., 2002. The Diagnostic Interview for Social and Communication Disorders: background, inter-rater reliability and clinical use. J. Child Psychol. Psychiat 43 (3), 307–325.